Experiments on the high-field thermoelectric and thermal properties of chromium

R. Fletcher*
Physics Department, Queen's University, Kingston, Ontario, Canada K7L 3N6
(Received 17 December 1984)

We take advantage of the high sensitivity of thermopower measurements to investigate the de Haas–Shubnikov oscillations in a Cr single crystal at fields up to 8 T. The increased resolution, compared to that offered by magnetoresistance measurements, allows more detailed information to be obtained on a major branch of frequencies and reveals new branches. By analyzing the peaks in the Fourier transforms, rough estimates are made of the breakdown fields for the various orbits; typical values are probably in the range of 0–40 T with most being in the region of 30 T. Measurements on the monotonic components of the electrical and thermal conductivities allow the lattice conductivity to be extracted. The result is compatible with those of the isoelectronic and isostructural elements Mo and W.

I. INTRODUCTION

The presence of a spin-density wave (SDW) in antiferromagnetic chromium has pronounced effects on the Fermi surface of Cr.[1] Large sections of the surface are thought to be eliminated and the new periodicities introduced by the incommensurate SDW reconnect the remaining pockets of holes and electrons via small energy gaps leading to a complex de Haas–van Alphen (dHvA) spectrum. The original dHvA data[2] were fitted by a model based on these assumptions, and more recently Reifenberger *et al.*[3] have reexamined the model in some detail and shown that most of the data can be explained in terms of the holelike ellipsoids at N. Although the high-field galvanomagnetic properties of Cr are in accord with the model,[4] less success has been obtained with the oscillations in the magnetoresistivity, i.e., the Shubnikov–de Haas (SdH) frequencies.[3,5] Only one SdH frequency branch corresponds to a dHvA branch. It may be noted that the oscillations in the density of states which give rise to the dHvA oscillations in the susceptibility will also be reflected as oscillations in most of the transport coefficients,[6] but the amplitude will be typically less than 1% of the monotonic part for the case of the magnetoresistivity. When the amplitude becomes significantly larger than this, as it does for some of the SdH oscillations in Cr[5], one usually suspects the presence of magnetic breakdown between the various sheets of the Fermi surface. Such breakdown can alter the trajectories of the electrons in an oscillating manner thus giving rise to large oscillations in the transport coefficients. Reifenberger *et al.*[3] have interpreted one of the SdH frequencies in terms of an interference orbit, a plausible suggestion since the orbit that they discussed would not be visible in the dHvA spectrum.

The intent of the present work is to use the increased sensitivity of thermopower (TEP) measurements to magneto-oscillatory phenomena in order to investigate the SdH oscillations in more detail. TEP gives identical information to resistivity with regard to quantum oscillations[7] but it is usually more sensitive in practical situations. The reason for this is that the TEP has its origin in the derivative of resistivity as a function of energy, which is closely related to the derivative as a function of magnetic field. Furthermore, at high fields the monotonic part of the TEP is usually of smaller magnitude than the oscillatory part, a feature which is very convenient from an experimental point of view. The only case where TEP measurements lack sensitivity is when the cyclotron effective mass m^* of the orbit is close to zero; such an orbit has little energy dependence, in particular with regard to resistivity. Since the orbit suggested by Reifenberger *et al.*[3] has a tiny effective mass $\sim 0.01 m_e$ it is of interest to determine whether it is present in TEP data.

In the course of this work sufficient data were taken on the monotonic parts of the electrical and thermal resistivities to enable the lattice conductivity of Cr to be extracted. Butler and Williams[8] have recently developed a theory which relates the electron-phonon enhancement factor to lattice conductivity, and the present data provide a useful addition in comparing their theory to experimental data.

II. EXPERIMENTAL DETAILS

The sample was in the form of a rectangular parallelepiped measuring about $6\times1\times1$ mm^3. It had been cut with its long axis parallel to a [001] direction and the large faces parallel to (110) planes. Two pieces of Pt foil, each about $2\times0.5\times0.25$ mm^3, were spot welded to the sample to act as potential and thermal probes. To these were soft soldered copper-clad NbTi wires (with the copper cladding removed over the last few centimeters) from the voltage detector, and also 220 Ω, $\frac{1}{8}$W Allan Bradley carbon resistors acting as thermometers. A current wire and a heater were soft soldered to one end of the sample; the other end was soft soldered to a copper block which was thermally connected to the He bath by a piece of flexible copper braid. The copper block was in turn screwed into a rotating sample holder.[9]

The arrangement was not ideally suited for thermal measurements, there being a relatively large thermal resistance between the sample and the helium bath which lim-

ited the heat current to $\lesssim 1$ mW. Fortunately the magnetothermal resistivity of the sample was generally high, otherwise the experiments might not have been feasible. The arrangement also suffered from a much larger electrical noise than is usually observed. This is thought to be a result of the relative looseness of the gear assembly which allowed small movements of the sample to take place. The problem was aggravated when the He bath was pumped, and so most of the present data were obtained with the bath near atmospheric pressure. This meant that orbits with masses greater than a few tenths of the electron mass were unlikely to be visible.

Most of the data were taken with the SDW wave vector **Q** oriented parallel to the long axis of the sample, i.e., **Q**||**U** where **U** is the heat current density. Under these conditions the resistance ratio $R_{293\,K}/R_{4.2\,K}$ was about 1500. The alternate orientation gave no extra information and seemed to be generally less sensitive to the oscillations. Because all the frequencies that were observed were rather low, long field sweeps were necessary for the best possible frequency resolution; usually a range of 3.6–8.0 T was used. Field B was swept so that B^{-1} was linear in time with data being taken at equal intervals in time. A single sweep took about 20–30 min.

On each cool down, the symmetry axis of interest was located using rotation curves of the magnetoresistance and TEP at about 7 T; this could be done to an accuracy of a few tenths of a degree. Field sweeps were then taken at various orientations of **B** relative to the sample axes, confining the measurements to the major symmetry planes. The accuracy with which the sample could be rotated in a symmetry plane was determined by the accuracy with which it was initially mounted in the cryostat (probably about 1°–2°). Thus, it was possible to start accurately at a symmetry axis, but by the end of the traverse the sample was misaligned by 1°–2°. This may be relevant since the amplitude of some of the components seemed to be sensitive to slight misalignments from the exact symmetry plane.

III. OSCILLATORY DATA ANALYSIS

Figure 1 shows three examples of Fourier transforms of data taken in the basal plane. Many of the peaks are well separated, but those at the lowest frequency and the one near 120 T have more than one component. A detailed study shows that when peaks overlap, then, even if they are resolved, the maxima do not necessarily accurately reflect the actual frequencies involved.[10] This is a common problem for these data and it becomes necessary to develop a procedure which enables the maximum amount of information to be obtained.

The shape of the peaks in the Fourier transforms is intrinsic and is determined by three factors: (i) The length of the data set, in terms of $1/B$, (ii) the way in which the amplitude of the data varies with B, and (iii), the choice of the envelope function used to suppress the side lobes in the transform that are caused by the abrupt start and finish of the data. The Appendix gives some details appropriate to the present case. Figure 2 shows examples of transforms calculated on the assumption that the data are of the form

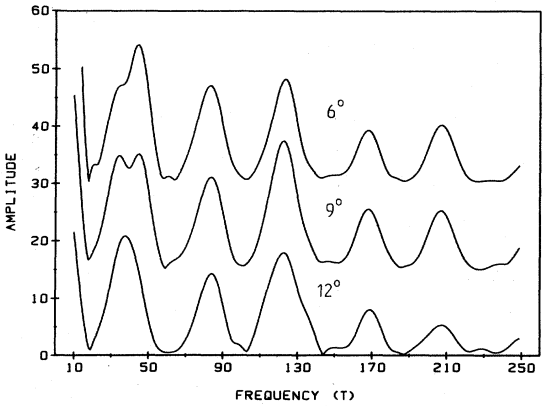

FIG. 1. Fourier transforms of data taken in the basal (plane D). The angles are measured from [100] towards [110]. The two peaks near 40 T are sometimes resolved and sometimes not, even though their spacing is relatively constant in this range of angles. The two peaks near 120 T (cf. Fig. 5) are never resolved. The amplitude scale is arbitrary.

$$F(B)=A\exp(-B_0/B)\cos\left[\frac{2\pi f_0}{B}+\phi\right], \tag{1}$$

where f_0 is the frequency of the oscillation, assumed to be 100 T in Fig. 2, and A,B_0, and ϕ are constants. The envelope function is chosen to be $1+\cos(\Omega/B)$ where Ω is such that it makes the envelope zero at each end of the data. When B_0 is equal to zero the transform has its minimum half width (at about 13.1 T for these data taking the starting field at 3.6 and the finishing field at 8.0 T). Two frequencies spaced closer than the half width will usually not be resolved; this is a rough guide since whether or not they are resolved in this region is also dependent on the relative phases of the two frequencies (see Ref. 10 for some examples). As B_0 increases so does the half width of the peak, and the residual side lobes rapidly disappear.

Much of the data were analyzed by fitting the

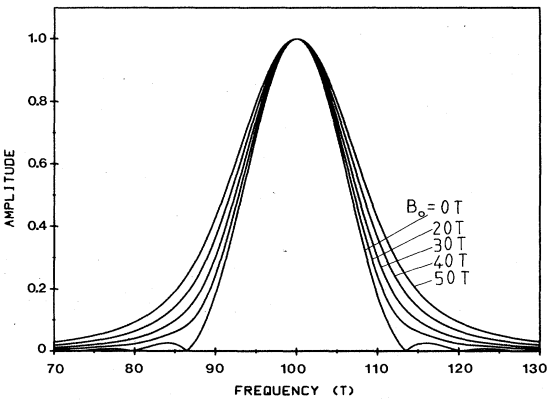

FIG. 2. Calculated transforms of Eq. (1) with an envelope function $[1+\cos(\Omega/B)]$, cf. Eq. (A4), for various values of B_0. The frequency f_0 is taken to be 100 T and the data spans the range of 3.6–8.0 T. The amplitudes are normalized to unity at $f=100$ T.

transforms to the theoretical curves [cf. Eq. (A4) of the Appendix] which required the use of four variables to represent each frequency component. Figure 3 shows an example of a fit to experimental data using four frequency components (and hence 16 unknowns). The fitted curve follows the data extremely well indicating that there are indeed only four components present within experimental error. Figure 4 shows an example of a single peak which cannot be accurately fitted by a single frequency. The shape of the peak, together with the angular variation of these and other data, suggests that two frequencies are present, and the upper curve of Fig. 4 is fitted with this assumption. This example illustrates the difficulties involved since one does not know *a priori* how many frequencies are present. In such cases one can only use the consistency of the results as a function of angle as the primary criterion for deciding on the number of components. One should also bear in mind that Eq. (1) might not be a good representation of the data. It is possible that an unusual dependence of amplitude on field for a particular frequency might yield a transform which could be mistaken for a number of discrete frequencies. In principle, selected ranges of the complex transform may be retransformed to yield the original data in the form of a filtered signal, but this procedure has not been carried out for the present data.

In many cases the peaks are sufficiently well resolved that fitting for purposes of obtaining the frequencies is superfluous. However, the fit does yield an estimate of the quantity B_0 in Eq. (1). Contributions to B_0 arise from three different sources. One expects a contribution from the effects of impurity scattering[11] since the Dingle factor is of the form $\exp(-2\pi^2 k_B T_D m^*/e\hbar B)$ where the constants have their usual significance and T_D is a constant with dimensions of temperature. If $m^* < 0.2m_e$ and $T_D < 1$ K (cf. results quoted later and Ref. 2), then this would give an effective $B_0 < 3$ T which would probably not be resolved in this work. A larger contribution is potentially possible through the usual temperature broadening factor $x/\sinh x$ with $x = 2\pi^2 k_B T m^*/e\hbar B$. For large x this factor tends to $2xe^{-x}$ and for

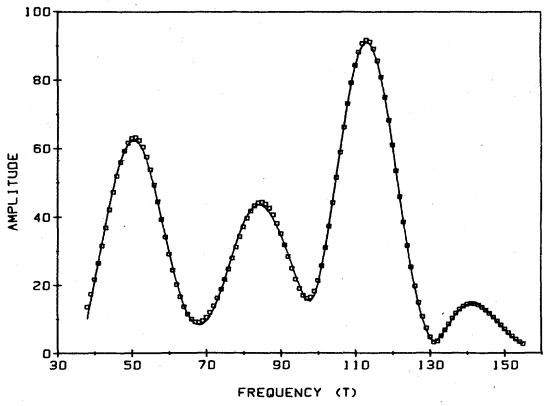

FIG. 3. A typical fit of the data to a sum of terms (in this case four) of the form shown in Eq. (A4); in this case the frequency components are well separated. The data were taken in the basal plane at 35° from [100] to [110]. The amplitude units are arbitrary.

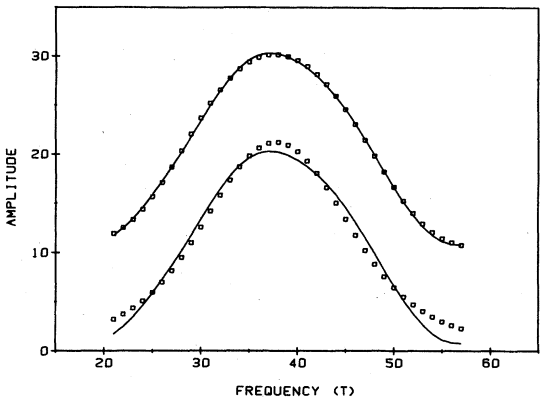

FIG. 4. An example of two fits to the same peak using one (lower curve) and two (upper curve) components. The upper curve is displaced vertically by 10 units for clarity. These are the same data as appear in the lowest curve of Fig. 1.

$m^* < 0.2m$ and $T \simeq 4.5$ K, $x < 13/B$. If the experiments had been carried out at lower T then this factor would again have been negligible since for $x < 1$ the factor $x/\sinh x$ saturates at unity. Finally, B_0 should reflect the breakdown fields required for the electrons to traverse the orbit under consideration (cf. Ref. 3). This must be the dominant contribution for many of the frequency components studied here since we regularly find values in the range of 35—50 T for B_0. As a check on the accuracy with which B_0 can be obtained, the data taken with B at 35° from [110] towards [001] have been analyzed using the width of the transform and also by fitting the original data to Eq. (1). (This procedure is essentially possible only here.) The former technique gives $B_0 = 47$ T and the latter, $B_0 = 49$ T. This good agreement is probably fortuitous in part because the analysis of the transforms as a function of angle is found to give random variations in B_0 of ± 5 T in good cases, and up to ± 10 T in poor cases.

IV. RESULTS AND DISCUSSION

A. Oscillatory results

Figure 5 shows the frequencies that have been detected in the present experiments using TEP measurements. The labeling of the planes is the same as that in Ref. 2. Although we do not observe some of the higher frequencies visible in the earlier SdH data[5] taken at fields of up to 20 T, Fig. 5 shows a richer spectrum than was previously obtained in this frequency range. Groups of frequencies near 500, 1000, and 1500 T are visible in the basal plane but were not investigated in detail because of low signal amplitude; these seem to be the branches seen by Graebner and Marcus[2] in the dHvA (and labeled ξ, σ, and λ by them) and also by Wallace and Bohm[12] and Snider and Thomas[13] in ultrasonic attenuation studies.

The branch labeled a (and presumably a_1), has been observed previously[3,5] and has been interpreted[3] as originating from an interference orbit on the hole ellipsoid chains at N. The present results suggest that this branch is more complex than was earlier thought to be the case. In plane C, the peak in the transform appropriate to a must be

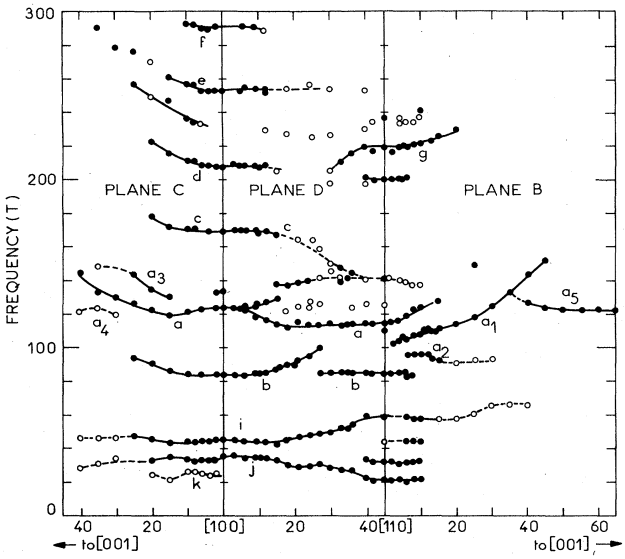

FIG. 5. Quantum oscillation frequencies versus magnetic field direction. The accuracy is better than ±1 T or ±1%, whichever is larger. The filled circles denote large amplitudes and clearly observed frequencies; the open circles are small amplitude components and less reliable.

augmented by other frequencies, a_3 and a_4, for angles beyond 15° from [100], through a always remains the strongest component; it is possible that the short branch near [100] at 133 T is part of a_3. At angles greater than 35°, the amplitude decreases rapidly and though a is visible up to 65° it is impossible to obtain accurate frequency values. The coefficient B_0 [see Eq. (1)] is very constant for branch a at 43±5 T from [100] to 35° from [100]. Using the measured effective mass $m^*\simeq 0.19m_e$ (see later) suggests a breakdown field of about 30 T for branch a.

The same branch is clearly visible through the basal (plane D) but reliable values of B_0 are not possible because of the presence of poorly resolved structure in the range of 120—130 T (cf. Fig. 5). At about 10° from [110], the amplitude of a rises rapidly and by [110] it is roughly five times larger than all other frequency components. This persists in plane B until about 4—5° from [110] where the amplitude drops very rapidly, and in the region of 6—10° from [110] all of a, a_1, and a_2 are of small amplitude, though a_1 begins to dominate here and is presumably the branch followed in the SdH work.[5] For angles $>15°$, a_1 has a value of $B_0=50\pm 8$ T with no obvious variation with angle. Again using the estimated effective mass (see below) of $m^*=0.15$—$0.20m_e$ suggests a breakdown field of 35—40 T. The lower branch a_5, which may intersect a_1 at about 35° from [110] has similar values of B_0; there is no doubt that a_5 is not the dHvA branch[2] labeled ω and seen in the SdH work.[5]

The present data allow some estimates of the effective mass to be made for branches a and a_1. At 30° from [100] in plane C, a_3 and a_4 have small amplitudes and the temperature dependence of a can be seen giving $m^*=(0.19\pm 0.02)m_e$. This is indistinguishable from the effective mass of the nearby dHvA branch labeled ϵ at $0.18m_e$. In plane B, a_1 can be seen reasonably clearly in both TEP and magnetoresistivity ρ_{xx}. By measuring their relative amplitudes, say $\tilde{S}$ and $\tilde{\rho}_{xx}$, the effective mass may be evaluated using the relation[7,14]

$$\tilde{S}=\left[\frac{\pi k}{e}\right]\mathscr{L}(X)(\tilde{\rho}_{xx}/\bar{\rho}_{xx})\,, \tag{2}$$

where $\mathscr{L}(x)$ is the Langevin function, with $x=(2\pi^2 k_B T m^*/\hbar eB)$, and $\bar{\rho}_{xx}$ is the monotonic part of the resistivity. In this way one finds m^* to be in the range 0.15—$0.20m_e$. This case is of further interest since the relative phases of $\tilde{S}$ and $\tilde{\rho}_{xx}$ indicate the nature of the orbit[7] as being holelike.[15,16] Reifenberger *et al.*[3] have suggested that a arises from an interference orbit on the hole ellipsoids at N and estimate an effective mass $m^*\simeq 0.01m_e$ near [100]. They argue that their own data and that of Arko *et al.*[5] are in agreement with this low effective mass in that the amplitude of the SdH oscillations does not appreciably change between 1.2 and 4.2 K. However, if $m^*=0.1m_e$, one would expect an increase in amplitude of only 12% in cooling from 4.2 to 1.2 K at 7 T, and for the results of Arko *et al.* taken at 15 T the changes would be about 3%. Such changes are likely to be too small to be observable suggesting that $m^*\simeq 0.1m_e$ is a reasonable lower limit for m^* as provided by their data. Along [100] changes of amplitude consistent with $m^*\simeq 0.1m_e$ are observed in the present data, but the resolution is not good enough to provide a reliable measure. However, a value of $0.01m_e$ seems to be inconsistent with the observed absolute amplitude of the TEP oscillations over the whole extent of branch a. Thus, for $x<1$, Eq. (2) reduces to

$$\tilde{S}\simeq\left[\frac{\pi k}{e}\right]\left[\frac{x}{3}\right]\left[\frac{\tilde{\rho}_{xx}}{\bar{\rho}_{xx}}\right] \tag{3}$$

at 7 T and 4.2 K, $x=0.09$ for $m^*=0.01m_e$ and taking $(\tilde{\rho}_{xx}/\bar{\rho}_{xx})\sim 0.01$ (unresolved oscillations in ρ_{xx} are always visible at this level for the present sample) predicts $\tilde{S}\sim 0.08\ \mu\mathrm{V\,K^{-1}}$. This is about an order of magnitude less than the observed values. Although these estimates apply to a mixture of frequencies (as do the arguments above of Reifenberger *et al.*[3]), branch a is observed to be one of the highest amplitude components and an order of magnitude discrepancy seems unlikely.

Thus, although the present data do support a holelike interpretation for a, they do not support the low effective mass required for the identification of Reifenberger *et al.*[3] Nevertheless, the fact that this branch is so strong in the transport measurements and absent in the dHvA data does support the hypothesis of an interference orbit. Indeed most of the branches seen in the present investigation have the same features. Although Graebner and Marcus,[2] and Reifenberger *et al.*,[3] have had remarkable success in explaining most of the dHvA branches in terms of the hole ellipsoids at N, one must bear in mind that only a relatively small fraction of the total Fermi surface is represented by these ellipsoids. If these surfaces are assumed to perfectly ellipsoidal with quadratic energy versus wave-vector dependence [an approximation that works well for Mo (Ref. 17) and W (Ref. 18)] with semimajor axes[3] of $\alpha=0.173\ \text{Å}^{-1}$, $\beta=0.234\ \text{Å}^{-1}$, and $\gamma=0.268\ \text{Å}^{-1}$, to-

gether with the estimate of the effective mass of the orbit having area $\pi\alpha\beta$ at $0.42m_e$, then one deduces a total contribution to the electronic specific-heat coefficient for six such ellipsoids of only 0.26 mJ mole^{-1} K^{-2}, compared to the total measured value[19] of 1.46 mJ mole^{-1} K^{-2}. Since Cr behaves as a compensated metal at not too high field,[4] an equal number of electrons per unit cell must be found. These could well be provided by the electrons at X but it seems unlikely that their effective mass could be large enough to produce the missing specific heat. Thus, there appear to be other pieces of Fermi surface, as yet undetected or unrecognized by the dHvA, which may also be relevant to the SdH oscillations. Arko *et al.*[4,5] suggest that the most likely origin of both their SdH and monotonic ρ_{xx} data is the hole surface at H which may partly persist after the onset of antiferromagnetism, since in principle breakdown is possible from this surface to the electrons at X thus causing Cr to become uncompensated, as is observed at high fields.

In the region of [100] the branches i, j, and k have frequencies similar to the dHvA branches[2] γ, β, and α, but their variation with angle seems to be different in plane D. Near [110], B_0 is found to be 30 ± 5 and 40 ± 5 T for i and j, respectively. In the same plane towards [100], B_0 drops to 15 ± 15 T for i and 25 ± 5 T for j. In plane C, B_0 remains small at 15 ± 5 T for i and 10 ± 10 T for j. It should be noted that in the region of [100], i and j are not resolved in the transforms and the reliability of B_0 must be in doubt.

The next largest amplitude branch is that labeled b; again Fig. 1 is representative of the amplitude. Values of B_0 lie in the range 40 ± 10 T. This branch in not visible in either dHvA or SdH work. The SdH data[5] suggest that a and a_1 are accompanied by higher-frequency branches which are almost harmonics. In these data e is close to the second harmonic, but the lack of agreement is well outside experimental error, especially when one examines the angular dependences. The same is true for g near [110]. As a matter of fact, c and e are closer to being the second and third harmonics of b but again the lack of agreement is outside experimental error. For c, the value of B_0 is 20 ± 7 T and for d is 45 ± 5 T. None of these branches shows any correspondence with dHvA data.[2]

At the present time there is no consistent interpretation for any of the branches that have been observed in these experiments.

B. Lattice conductivity

For currents parallel to **Q** and perpendicular to **B** the transverse electrical and thermal resistivities ρ_{xx} and γ_{xx} are very high, and at the highest fields the lattice conductivity λ_g becomes significant. The presence of open orbits along **Q** complicates the analysis but λ_g can be obtained as follows. Since there is only one direction of open orbit (along x) we can then approximate the electrical conductivity in the xy plane by[20]

$$\sigma_{ij}=\begin{vmatrix}(b_1/B^2) & (c/B)\\ -(c/B) & (b_2/B^2)+d\end{vmatrix}, \tag{4}$$

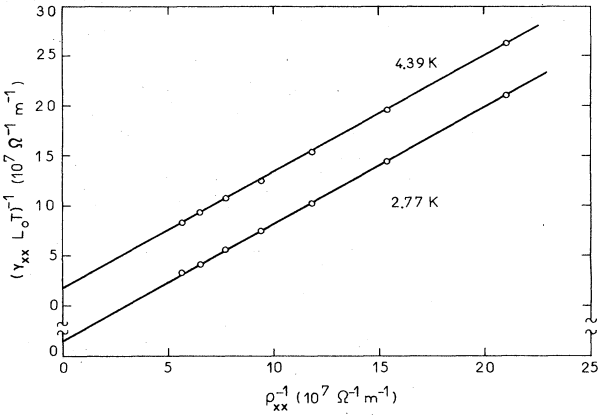

FIG. 6. Data on the monotonic parts of ρ_{xx} and γ_{xx} taken for $\mathbf{B}\|[110]$ and plotted in the form of $(\gamma_{xx}L_0T)^{-1}$ against ρ_{xx}^{-1}. According to Eq. (7) the lines should be reasonably straight with intercepts of λ_g/L_0T. The data spans the approximate field range of 3.6—8.0 T.

where d represents the open-orbit contribution and b_1,b_2, and c the conductivity of the closed surfaces. Ignoring the other components is strictly valid only along an axis of threefold or higher symmetry, but these components will probably be negligible provided the open surface is reasonably free of corrugations[20] (this latter assumption is supported by the galvanomagnetic data[4]); Eq. (4) gives

$$\rho_{xx}=(b_2+dB^2)/(db_1+c^2+b_1b_2/B^2)\ . \tag{5}$$

The thermal conductivity of the electrons λ_{ij} is assumed to be of the same form as σ_{ij}, i.e., $\lambda_{ij}=L_0T\sigma_{ij}$ where L_0 is the Sommerfeld value of the Lorenz number, which should be appropriate since the crystal is well into the residual resistance regime by 4.2 K. λ_g is assumed to be isotropic; this is not essential and one can show that the quantity determined here is that appropriate to phonon

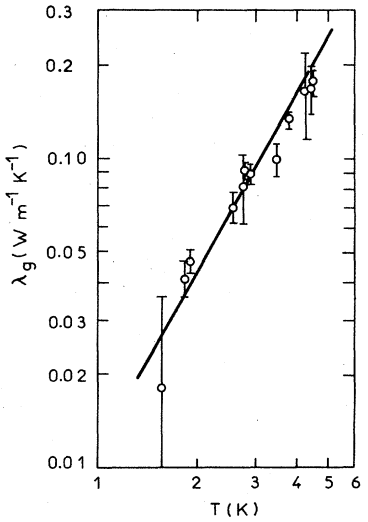

FIG. 7. The lattice conductivity λ_g plotted against T. The straight line is $\lambda_g=\alpha T^2$ with $\alpha=0.010_5\pm0.004$ W m^{-1} K^{-3}.

conduction parallel to **Q**. With these assumptions[21] one finds

$$\gamma_{xx}=[b_2'+(\lambda_g+d')B^2]/[\lambda_g(b_1'+b_2')+\lambda_g(d'+\lambda_g)B^2 +c^2+(b_1'b_2'/B^2)] , \quad (6)$$

where $b_1'=L_0Tb_1$, etc. As $B\to\infty$, $\gamma_{xx}\to 1/\lambda_g$. Fortunately the expression simplifies when one considers the relative magnitudes of d' and λ_g. With the current **J**||[001], **Q**||[100], and **B**||[010], the present measurements indicate a saturation value of $\rho_{xx}\simeq 10$ nΩm at 5 T, and this should be approximately the magnitude of d^{-1}. Thus, $d'=L_0Td\simeq 10$ W m^{-1}K^{-1} at 4.2 K. By contrast $\lambda_g\simeq 0.2$ W m^{-1}K^{-1} at the same temperature so that $d'\gg\lambda_g$. Hence Eq. (6) becomes

$$\gamma_{xx}^{-1}=L_0T\rho_{xx}^{-1}+\lambda_g(d'B^2+b_1'+b_2')/(b_2'+d'B^2) . \quad (7)$$

The data of Arko *et al.*[4] [their Fig. 4(b)] for **J**||[001] and **Q**||**B**||[100] is appropriate to closed orbits so that $\rho_{xx}\simeq b/B^2$ where $b\simeq b_1\simeq b_2$. These data were obtained on a crystal of similar purity to that used here, so we can use this to estimate $b\simeq 3\times 10^8$ T^2 Ω^{-1} m^{-1} and hence $b_1'\simeq b_2'\simeq L_0Tb\simeq 30$ W T^2 m^{-1}K^{-1} at 4.2 K. Thus, at lower fields the second term in Eq. (7) may exhibit some B dependence but at high fields ~ 8 T it should be accurately equal to λ_g. [At 2 T the multiplier of λ_g in Eq. (7) has a value of about 1.5.] Figure 6 shows examples of γ_{xx}^{-1} plotted against ρ_{xx}^{-1}. The absence of significant curvature supports the above assumptions and suggests that the intercepts can be identified with λ_g. Incidentally, all the data were obtained for **B**||[110] because this gives the highest values of ρ_{xx} as a function of **B** [cf. Figs. 6(a) and 6(b) of Ref. 4]. The slopes of the lines, which should be L_0T, are always too high by a factor of 1.25 ± 0.05; the most likely explanation is that the electrical and thermal lengths of the sample are not identical, a situation which is probably not unexpected since the probes are less than 3 mm apart and the width of the probes is comparable to their separation.

The intercepts of Fig. 6 and other similar data are shown in Fig. 7 as a function of T. The data are not inconsistent with a temperature dependence of the form $\lambda_g=\alpha T^2$, as would be appropriate to electron-phonon scattering, with $\alpha=0.010_5\pm 0.004$ W m^{-1}K^{-3}. There seems to be no previous experimental work with which to compare this result.

Butler and Williams[8] have recently derived an equation relating λ_g and λ, the electron-phonon mass enhancement factor, i.e.,

$$W_{e\text{-ph}}(T/\Theta_D)^2(\lim T\to 0)=0.42\Omega_a^{1/3}N\lambda , \quad (8)$$

where $W_{e\text{-ph}}=\lambda_g^{-1}$ in the present case, provided dislocation scattering is not significant (and with λ_g in W cm^{-1}K^{-1}), Θ_D is the Debye temperature, Ω_a the atomic volume in Å^3, and N the band density of states at the Fermi energy for 1 spin (in eV^{-1} atom^{-1}). For the present purposes we rewrite Eq. (8) as

$$X=0.42\alpha\Omega_aN\lambda\Theta_D^2 , \quad (9)$$

where α is the coefficient of T^2 found for λ_g (in W cm^{-1}K^{-3}) and X is a numerical factor which will be unity if Eq. (8) holds. Using the measured[19] specific-heat coefficient of 1.46 mJ mole^{-1}K^{-2} gives $N=0.31/(1+\lambda)$ states eV^{-1} atom^{-1}. The parameter λ is not well known for Cr but a recent calculation[22] puts it in the range of 0.5–0.83. Using[19] $\Theta_D=598$ K, $\Omega_a^{1/3}=2.29$ Å, and $\alpha=1.1\times 10^{-4}$ W cm^{-1}K^{-3} gives $X=4.5$ with an uncertainty of about 50%. For comparison purposes one can estimate X for Mo and W. In the case of W (Ref. 19), $N=0.26/(1+\lambda)$ eV^{-1} atom^{-1}, $\Theta_D=388$ K, $\Omega_a^{1/3}=2.51$ Å, $\lambda=0.28$ (Ref. 8), $\alpha=3.8\times 10^{-4}$ W cm^{-1}K^{-3} (Ref. 23) to give $X=3.4$. For Mo (Ref. 19), $N=0.44/(1+\lambda)$ eV^{-1} atom^{-1}, $\Theta_D=4.59$ K, $\Omega_a^{1/3}=2.50$ Å, $\lambda=0.41$ (Ref. 8), and $\alpha=2.2\times 10^{-4}$ W cm^{-1}K^{-3} (Ref. 24) to give $X=6.3$. Although the values of X are well above unity showing that the theory underestimates λ_g, all the results are similar and appear to be consistent for these metals. It seems[8] that $X=2$ is more typical of the other metals which have been investigated.

V. SUMMARY

Thermopower measurements have been used to investigate the quantum oscillations in Cr. Because the oscillations are visible at lower fields as compared to SdH measurements, the present experiments have provided a better frequency resolution than before. This illustrates the sensitivity of thermopower very well since the highest magnetic field available in this work is much less than that used in the SdH studies. As well as obtaining new information about previously observed branches, several new frequency branches have been detected. It has proved possible to estimate the effective mass of one of the most visible branches, giving a value close to that obtained for a nearby dHvA branch. This is contrary to the prediction of Reifenberger *et al.*[3] who suggested an interference orbit of very low effective mass as the source of this branch. Estimates of the breakdown field for various frequencies are in the range of 0–40 T with most being in the region of 30 T.

By simultaneously observing the thermopower and resistivity oscillations, preferably for fields above 10 T to obtain a good signal-to-noise ratio in the latter, it should be possible to measure the effective masses and determine the nature of the orbits involved, i.e., hole or electronlike, for many of the observable frequencies. It seems certain that many more frequencies will become visible in thermopower measurements at higher fields, especially if the temperature is reduced to below 4.2 K.

The present experiments have also yielded an estimate of the lattice conductivity of Cr at low temperatures. The magnitude is similar to that observed in Mo and W when scaled by appropriate parameters.

ACKNOWLEDGMENTS

Dr. D. Morrison of the Department of Nuclear Engineering, University of Arizona, deserves special credit for supplying the chromium crystal and rotating sample holder, and also for useful conversations and communications concerning data analysis. The invaluable help of Mr. J. Ungar with data analysis is warmly appreciated.

The work was made possible by a grant from the Natural Science and Engineering Research Council of Canada.

APPENDIX

It is convenient to use t and ω as variables. In the case of quantum oscillations $t=B^{-1}$ and $\omega=2\pi f$ where B is the flux density and f the frequency of the quantum oscillations. For a single sinusoid, $F(t)=\cos(\omega_0 t+\phi)$, the Fourier transform over the range $-T<t<T$ is given by

$$g(\omega)=\int_{-T}^{T} e^{-i\omega t}\cos(\omega_0 t+\phi)dt = \frac{e^{i\phi}\sin(\omega_0-\omega)T}{(\omega_0-\omega)}+\frac{e^{-i\phi}\sin(\omega_0+\omega)T}{(\omega_0+\omega)}\ , \quad \text{(A1)}$$

provided $\omega_0 T>>\pi$, the second term is very small near ω_0 and we have ignored it since this saves a factor of 2 in computing time. When $F(t)$ is modified by an exponential factor α ($=B_0$ in the body of the paper), i.e., $F(t)=e^{-\alpha t}\cos(\omega_0 t+\phi)$, then ω is replaced by $\omega+i\alpha$ so that

$$g(\omega)=e^{i\phi}\sin(\omega_D T)/\omega_D\ , \quad \text{(A2)}$$

where $\omega_D=\omega_0-\omega-i\alpha$. In this case

$$|g(\omega)|^2=\{\sin^2[(\omega_0-\omega)T] + \sinh^2(\alpha T)\}/[(\omega_0-\omega)^2+\alpha^2]\ , \quad \text{(A3)}$$

an equivalent expression has been given by Wallace and Bohm.[12] However, it should be noted that $|g(\omega)|^2$ does not show a split peak centered at $\omega=\omega_0$ as suggested by them; on the contrary, the maximum of $|g(\omega)|^2$ always occurs at $\omega=\omega_0$ and $|g(\omega)|^2\geq T^2$ for $\alpha\geq 0$.

In the present work we have used an envelope function of the form $[1+\cos(\Omega t)]$, where $\Omega=\pi/T$, chosen to suppress the side lobes which are a problem with Eq. (A2). Since

$$[1+\cos(\Omega t)]\cos(\omega_0 t+\phi)=\cos(\omega_0 t+\phi) + \tfrac{1}{2}[\cos(\omega_0 t+\phi+\Omega t) + \cos(\omega_0 t+\phi-\Omega t)]\ ,$$

then the new transform $g'(\omega)$ is simply the sum of the three terms like Eq. (A2) and is found to be

$$g'(\omega)=\frac{e^{i\phi}\sin(\omega_D T)}{\omega_D[1-(\omega_D/\Omega)^2]}\ . \quad \text{(A4)}$$

When $\alpha=0$, $|g'(\omega)|=T$ at $\omega=\omega_0$ and the half width $\Delta\omega$ is just 2Ω [or $\Delta f=2/(B_1^{-1}-B_2^{-1})$ where B_1 and B_2 are the starting and finishing fields]. Figure 2 shows examples of $|g'(\omega)|$ calculated for α ($=B_0$) in the range 0–50 T. For $\alpha\neq 0$, $|g'(\omega)|>T$ but the graphs have been normalized to unity at $\omega_0=\omega$ for comparison purposes.

The effect of shifting the range from $-T<t<T$ to $a<t<b$ is simply to introduce a factor $e^{i\omega_D T_0}$ where $T_0=(a+b)/2$. The phase factor $e^{i\omega T_0}$ is relevant if one wishes to find absolute phases, but our data are probably not accurate enough to warrant this. The remaining factor $e^{-\alpha T_0}$ varies rapidly with α and it was found much more convenient (and computationally faster) to fit the Fourier transforms with expressions like Eq. (A4), i.e., without the factor $e^{-\alpha T_0}$. This factor can be reinserted later if the absolute amplitudes of the original waveform are required. In the case of two or more overlapping peaks it is essential to retain the phase factors given in Eqs. (A2) or (A4) since these result in interference effects (cf. Ref. 10). In this case there are generally four unknowns for each frequency present i.e., A (the absolute amplitude), ω_0, α, and ϕ.

*Present address: Max-Planck-Institut fuer Festkoerperforschung, Hochfeld-Magnetlabor, Grenoble, France.

[1]W. M. Lomer, in *Proceedings of the International Conference on Magnetism, Nottingham, 1964* (IOP, London, 1965), p. 127.
[2]J. E. Graebner and J. A. Marcus, Phys. Rev. **175**, 659 (1968).
[3]R. Reifenberger, F. W. Holroyd, and E. Fawcett, J. Low Temp. Phys. **38**, 421 (1980).
[4]A. J. Arko, J. A. Marcus, and W. A. Reed, Phys. Rev. **176**, 671 (1968).
[5]A. J. Arko, J. A. Marcus, and W. A. Reed, Phys. Rev. **185**, 901 (1969).
[6]A. B. Pippard, Rep. Prog. Phys. **23**, 176 (1960).
[7]R. Fletcher, J. Low. Temp. Phys. **43**, 363 (1981).
[8]W. H. Butler and R. K. Williams, Phys. Rev. B **18**, 6483 (1978).
[9]G. F. Brennert, W. A. Reed, and E. Fawcett, Rev. Sci. Instrum. **36**, 1267 (1965).
[10]G. N. Kamm, J. Appl. Phys. **49**, 5951 (1978).
[11]A. V. Gold, in *Solid State Physics,* edited by J. F. Cochran and R. Haering (Gordon and Breach, New York, 1968), Vol. 1, p. 39.
[12]W. D. Wallace and H. V. Bohm, J. Phys. Chem. Solids **29**, 721 (1968).
[13]D. F. Snider and R. L. Thomas, Phys. Rev. B **3**, 1091 (1971).
[14]R. Fletcher, Phys. Rev. B **28**, 1721 (1983).
[15]Alekseevskii and Nizhankovskii (see Ref. 16) report no difference in the relative phases of TEP and ρ_{xx} oscillations from hole and electronlike surfaces. In the present case the phase of the TEP oscillations is different by π from the case of Al (Ref. 14) where the oscillations originate from an electronlike surface.
[16]N. E. Alekseevski and V. I. Nizhankovskii, Zh. Eksp. Teor. Fiz. **83** 1163 (1982) [Sov. Phys.—JETP **56**. 661 (1982)].
[17]J. A. Hoekstra and J. L. Stanford, Phys. Rev. B **8**, 1416 (1973).
[18]D. Sang, A. Myers, and P. J. Feenan, Solid State Commun. **35**, 27 (1980).
[19]K. A. Gschneider Jr., in *Solid State Physics,* edited by F. Seitz and D. Turnbull (Academic, New York, 1972), Vol. 16.

[20]A. A. Abrikosov, in *Solid State Physics,* edited by H. Ehrenreich, F. Seitz, and D. Turnbull (Academic, New York, 1972), supplement to Vol. 12.

[21]It is not clear whether Cr will show any magnetic contribution to the heat transport. This possibility has been ignored in this work.

[22]D. G. Laurent, J. Callaway, J. L. Fry, and N. E. Brener, Phys. Rev. B **23**, 4977 (1981).

[23]R. Fletcher, Philos. Mag. **32**, 565 (1975).

[24]R. Fletcher, Phys. Rev. **14**, 4329 (1976).